



## **Thermal Choking Transients in Coaxial Supersonic Combustor**

*Bu-Kyeng. Sung<sup>1</sup>, Jeong-Yeol. Choi<sup>1</sup>*

### **Abstract**

Numerical study is carried out to investigate the characteristics of supersonic turbulent combustion in Dual Combustion Ramjet(DCR) engine using a multi-dimensional 5th-order high resolution scheme. Two series of numerical experiment are carried out for the DCR combustors with various divergence angles and the length of the constant area combustor section. Operating conditions are selected by considering the flight conditions. Two different combustion modes are found by the investigation of the results depending on the formation of Mach reflection. It is analyzed that the relation between the turbulent combustion and the formation of the Mach reflection by the variation of scalar dissipation rate. Dynamic characteristics the turbulent supersonic combustion were investigated by the variation of wall pressure compared with other properties. Critical conditions for the combustion stabilization are reasoned from the characteristics of the turbulent combustion. The detailed mechanism of coupling between the compressibility effects and the turbulent combustion is understood as they are supporting with each other, similarly in detonation phenomena

**Keywords:** Dual Combustion Ramjet, Supersonic combustion, Non-premixed turbulent combustion, Scalar dissipation rate, Thermal-choking

### **1. Introduction**

The successful flight test of X-51A opened a new era of powered hypersonic flight for practical applications. A technology that distinguishes X-51A from previous scramjet flight test is the dual-mode ramjet (DMR) engine using liquid fuel. The DMR engine starts at thermally choked ramjet mode at supersonic launching speed, and then accelerates to hypersonic cruising condition, operating at scramjet mode. The DMR could have a practical flight range and time by the use of liquid fuel. The liquid fuel flows through the regenerative cooling passage, and then the superheated fuel is injected into the combustor at gas phase[1,2]. While the DMR would be attractive for reusable system, dual combustion ramjet (DCR) by Billig et al.[3] would be a more affordable concept for expendable system,. Fig. 1 is the schematics for DCR operation. A part of the incoming air is compressed to subsonic condition for very fuel-rich combustion in the gas generator. The pre-burned fuel is delivered to the supersonic combustor at high speed. The high temperature gaseous fuel mixes with the supersonic air and burns quite easily. Thus, the fuel-air mixing at the supersonic turbulent shear layer is the key factor of the combustion in the DCR engine, as well as in the rocket-based combined cycle (RBCC) engine.

Some of the supersonic combustion studies employing the co-flow of fuel and air can be related to the combustion in DCR[4~7], even though the efforts are taken in understanding the compressibility effects and the global structure of the supersonic combustion. Regardless of long time researches, the role of turbulence structures in supersonic combustion characteristics is becoming understood recently by the advances in computing capabilities and visualization techniques. In the present study, the behavior of the supersonic turbulent combustion in DCR is examined to perceive the stability in combustion dynamics by means of high resolution numerical analysis developed and validated as accompanying paper.

---

<sup>1</sup> *Department of Aerospace Engineering, Pusan national University, Busan 46241, Korea*

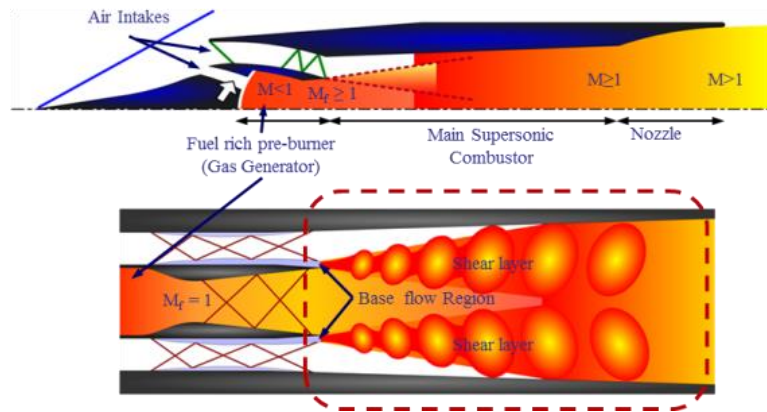


**Fig. 1** Flow schematics in DCR engine

## 2. DCR Combustor Model

### 2.1. Operating Conditions and Configurations of DCR

Pre-burning of heavy hydrocarbon liquid fuel with a small amount of air would be a brilliant idea to burn the fuel in supersonic flows. It is known that the optimum air ratio is approximately 1:3 for the pre-burner and the main supersonic combustor. Therefore, the equivalence ratio in the pre-burner is greater than 3.0 to maintain the equivalence ratio less than 1.0 in the main combustor. In this circumstance, the pre-burned gas mainly contains carbon monoxide and hydrogen of nearly same volumetric ratio with exit temperature around 1,000 K. The cracked fuel composition at such high temperature improves the combustion efficiency drastically even in the harsh condition for combustion in supersonic flow.

The coaxial fuel and stream for supersonic combustion is contemplated for by assuming the pre-burning of heavy hydrocarbon fuel,  $C_nH_{2n}$ . The final product at the exit of the preburner comprises of  $CO+H_2+1.88N_2$ , assuming the equivalence ratio of 3.0 in the pre-burner. For simplicity, the pre-burned fuel is injected into the supersonic combustor through the sonic nozzle at static temperature and pressure of 1,200K and 0.2 MPa, respectively, and the air ( $O_2+3.76N_2$ ) flows through the diffuser inlet at Mach 2.0 with the same static temperature and pressure. This condition roughly corresponds to the flight Mach number 6 at altitude of 20~30 km depending on the intake design and performance.

Accounting to the realistic engine size, the fuel port radius  $R$  (2.54 cm) with the lip thickness  $R$ , separating fuel and air stream, the main combustor radius  $3R$  and the length of the main combustor  $100R$  are presumed. Two different combustor configurations are considered for parametric studies of flame stabilization. The one is the divergent combustor with various divergent angle  $\theta$ , where  $\theta$  is changed from 0 to  $\tan^{-1}(9/1,000)$  and the other with the constant area combustion section of length  $L_c$ , where  $L_c$  is varied from 0 to  $90R$ . The exit radius of  $4R$  is assumed for the combustor, which corresponds to the divergent angle of  $\tan^{-1}(10/1,000)$  for the case where  $L_c = 0$ . The Fig.2 illustrates the flow conditions and configurations in detail.

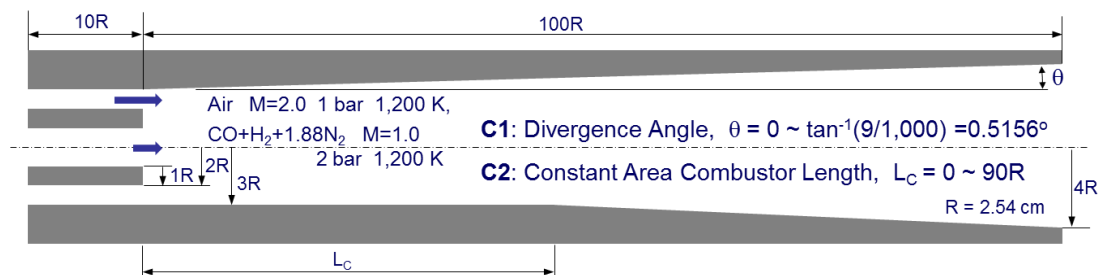


**Fig. 2** Configuration and flow conditions of DCR supersonic combustor

## 2.2. Numerical Modeling of DCR

The turbulent combustion is analyzed through the solution of the fully coupled governing equations of species, momentum and energy conservation equation with a hybrid RANS/LES turbulence model. Further details of the physical models and the solution procedures have been discussed in the previous paper. Only the differences will be stated, since almost the same strategy is used in this study including the multi-dimensional 5th-order accurate oMLP scheme.

The combustion model used in this study includes eight reacting species (CO, CO<sub>2</sub>, O, O<sub>2</sub>, H, H<sub>2</sub>, OH, H<sub>2</sub>O) and inert nitrogen (N<sub>2</sub>). The high temperature CO/H<sub>2</sub> oxidation mechanism obtained from Singh and Jachimowski. The Reynolds number based on the injector diameter is  $2.05 \times 10^5$ . The computational grid for Fig.2 is listed as follows; 2401×221 for main combustor, 97×81 for air inlet and 97×61 for fuel inlet. The computational grid is clustered at the wall surface while the uniform grid spacing is maintained around the former half of the combustor using 3/4 of grid points and longitudinally extended grid is built in the divergent section using 1/4 of grids. Time integration is carried out for 300,000 time steps by using CFL number of 2.0, while maximum of 4 sub-iterations are allowed at each time-step. The time step corresponds to 67.0 ns and physical computing time to 20.1 ms. Finally, Time averaging is carried out for later half of 150,000 time steps.

As a preliminary step for further investigation, the combustion efficiency of the time averaged result was checked at the combustor exit for the case of  $L_c = 50R$ . Fig. 3 is the summary of the combustion efficiency using four levels of different grid with three different schemes. In case of MUSCL3 scheme, the combustion efficiency remains low for all grid system It is interesting that the Level 1 (coarse) grid shows the best value while the combustion efficiency is lowered by the use of finer grids, but is recovered using finest (Level 4) grid. It is understood that the larger numerical diffusion in coarse grid, facilitates the mixing and combustion, resulting the coarse grid solution seeming to have better combustion characteristics. The combustion efficiency from WENO5 scheme demonstrates more monotonic variation since the combustion efficiency gets higher as the grid resolution gets finer. However, improvement in combustion efficiency is slowing down and it is limited to 0.8 even with finer grid refinement among the studied.

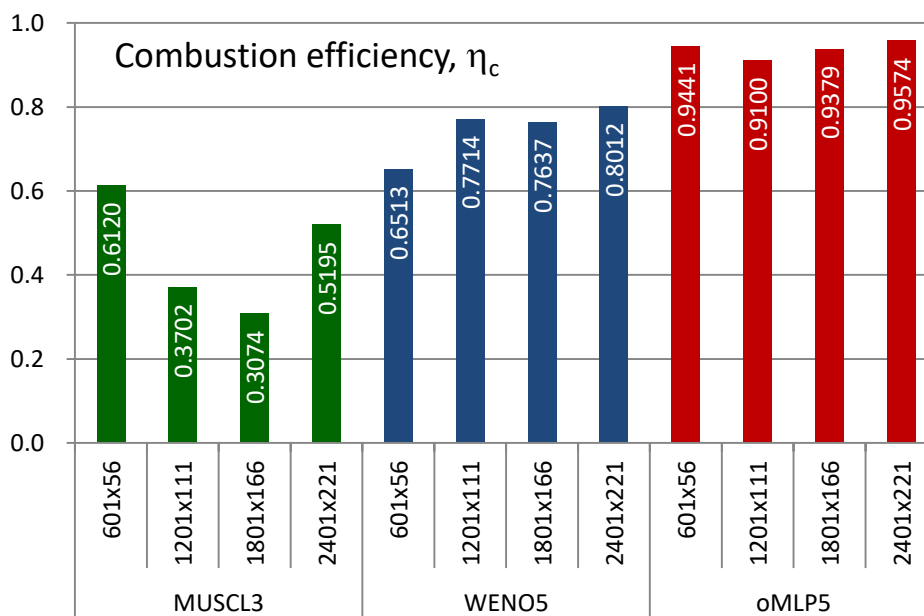


**Fig 3.** Combustion efficiency obtained by three high resolution schemes and four levels of grids for a DCR supersonic combustor of  $LC = 50R$

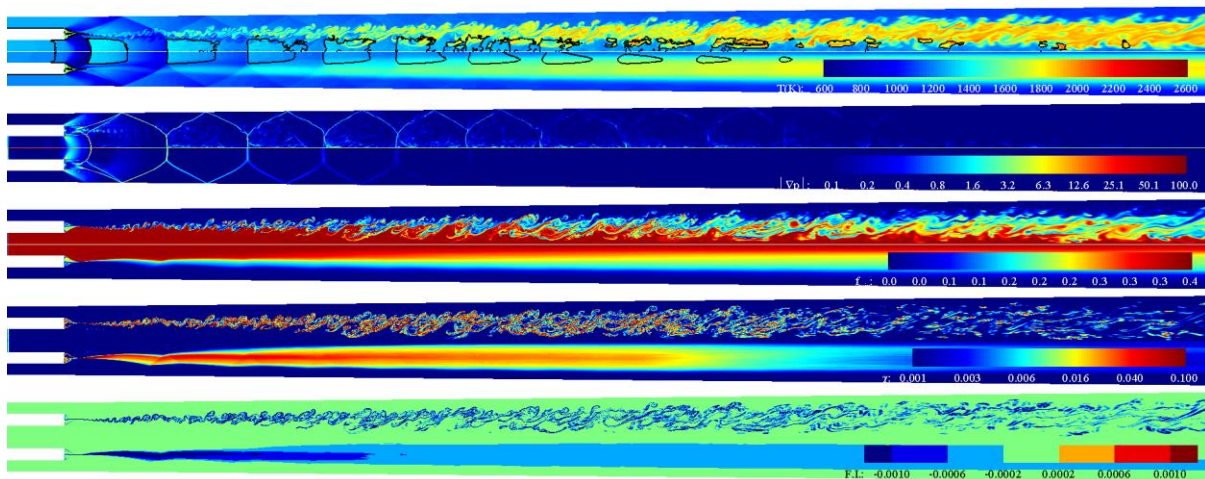
The advantage of the multi-dimensional higher order capability of oMLP scheme is clearly demonstrated in this result. Regardless of the grid resolution the combustion efficiency is well maintained above 0.9 or much higher than other schemes in average. It is to note that in case of Level 4 grid combustion efficiency of 0.95 is achieved pertaining complete combustion. An interesting point is the degradation

of the combustion efficiency is observed in the intermediate grid. It is interpreted that the numerical diffusion results in the better combustion characteristics at coarse resolution solution, even in the case of the multi-dimensional scheme.

### 3. Turbulent Combustion Characteristics in DCR

#### 3.1. Dynamic Features and Combustion Modes

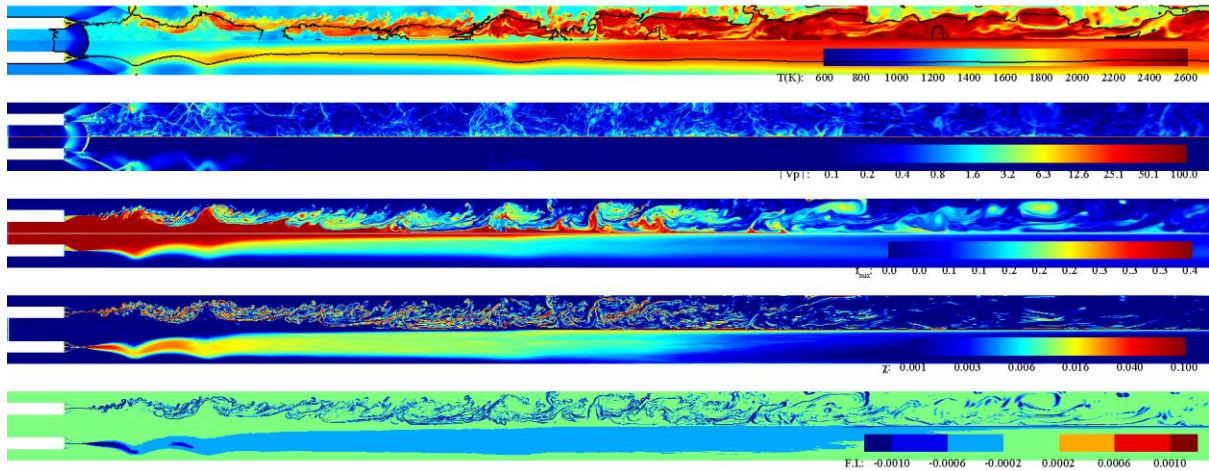
A series of parametric studies have been carried out to investigate the effect of the combustor divergence angle in the previous study[9]. Among the cases investigated, to investigate the transient period of thermal choking extreme two cases are selected. Fig. 4 and 5 are the results of two extreme cases showing instantaneous and time-averaged plots for temperature, density gradient, mixture fraction, scalar dissipation rate (SDR,  $\zeta$ ) and flame index (FI)[11,12]. Sonic line is overlaid with the temperature distribution as black solid line. For the case of divergent combustor in Fig. 4, the basic characteristics of shear layer development is similar to the validation case studied by Choi et al.[10] Higher Reynolds number than the validation case results in much more irregular Kelvin-Helmholtz instabilities, further developing as turbulent eddy motions. Difference of Mach number between the air and fuel flow makes more distinct pattern of shock train with Mach disks. At the beginning of the shock train, strong shock wave interacts with the turbulent shear layer while distorting the distribution of SDR and other variables. However, the strength of the shock wave is getting weaker as going downstream, and the interaction with the shear layer becomes unnoticeable accordingly. The SDR is high at the beginning, but becomes lower and wider for better combustion. It is found from the temperature distribution that the flame is developing very long, inversely with the decrease of the SDR. It is considered that some amount of fuel is flowing out of the combustor at unburned state. An interesting point is that FI is always negative along the shear layer. That is, the combustion is held in diffusive mode, differently from the validation case where premixed combustion is observed. It is reasoned that the fuel and air react promptly as they mix, since the temperature is sufficiently high for both sides, while the fuel is cold in the validation case.



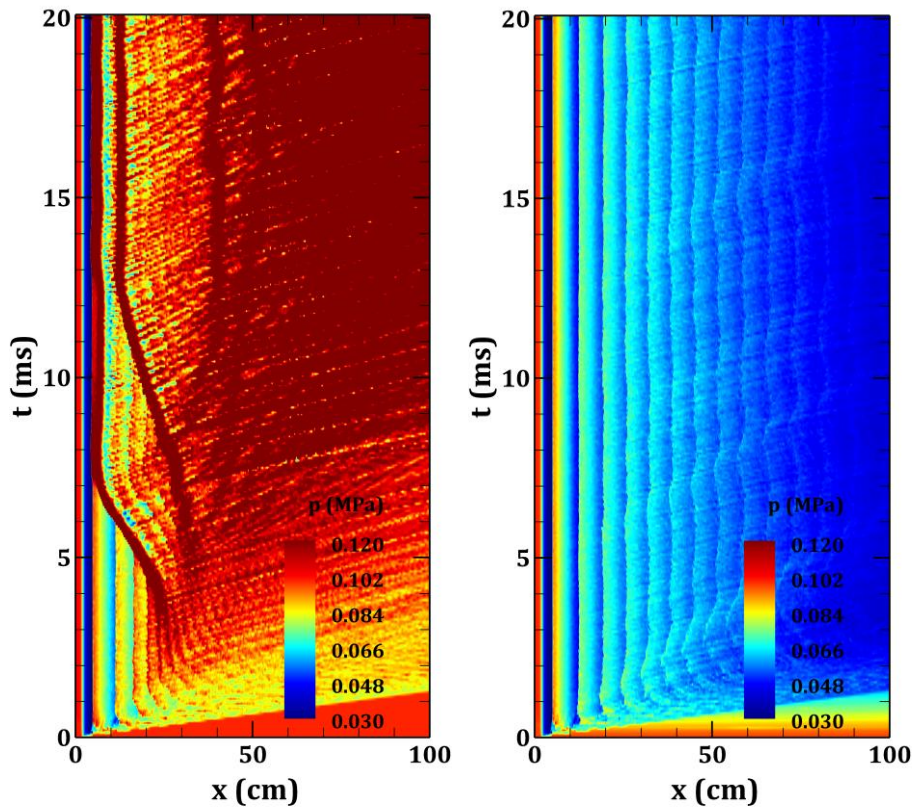
**Fig 4.** Instantaneous(upper) and time-averaged(lower) plots of flow variables for  $\theta = \tan^{-1}(9/1,000)$

Figure 5 is the result for a constant area combustor. It is found that the combustion is much stronger and almost all the fuel is consumed before exiting the computational domain. It could be a reason of compression effect by the reduced divergence angle makes the high temperature and pressure for better combustion. The changes in thermodynamics properties by the area change would be limited to small, since the maximum area ratio for both cases 1.69 at the combustor exit. Therefore, it is not considered as sufficient to account for such a drastic change regardless of the differences in divergence angle. By the close examination of the flame developing process from the beginning of injection, it is found that there are pressure wave interactions generated by the turbulence motion with heat addition at the middle of the combustor. The pressure wave interaction finally couples to the Mach reflection at

the combustor wall, which makes a thermal choking locally. By the presence of Mach reflection, the SDR becomes lower by the slowdown of flow speed, and the combustion is enhanced greatly. By the heat addition behind the Mach reflection, the normal shock wave moves forward closely to the injector lip. Finally, the flow is stabilized as shown in Fig. 6 after some transient period. Therefore, it is concluded that the coupled effects of compressibility and turbulent flame structures changes the mode of combustion to thermal choking, at least locally or instantaneously.



**Fig 5.** Instantaneous ( $t=5\text{ms}$ , upper) and time-averaged(lower) plots of flow variables for  $\theta = 0$



**Fig 6.** Pressure-time histories along the tube wall  $\theta = 0$  (left) and  $\theta = \tan^{-1}(9/1,000)$  (right)

### 3.2. Combustion Enhancement of the Constant Radius Combustor

To investigate the combustion enhancement of the constant radius combustor, the scatter plot of OH mass fraction and the FFT frequency analysis of wall pressure history is used. Figure 7 shows the scatter plots of time averaged OH mass fraction as a function of the axial distance from the gas generator colored by scalar dissipation rate and the flame index. The tendency of OH mass fraction distribution which implies the active reaction zone of the case  $\theta=0$  is the opposite of the one of case  $\theta = \tan^{-1}(9/1,000)$ . Due to the turbulent eddy motion accompanied by the compression effect, it is evident that the fuel and oxidizer are actively mixed right downstream of the gas generator. Consequently, the active reaction zone is formed at the upper half of the combustor, while the diverging combustor's reaction zone enlarged by flowing downstream. By looking at the scatter plot of the flame index, in the case of  $\theta=0$ , there is some area where the positive product of the spatial gradient of the fuel and oxidizer implies better fuel-air mixing. Even though this region is located at a small OH concentration, the effect of compressibility-turbulent motion is certainly visible. As mentioned above, due to the presence of Mach reflection which causes local thermal choking, the SDR can be greatly lowered compared with the diverging combustor as marked in the plot. Therefore, this effect of compressibility-turbulent eddy motion is confirmed to promote combustion efficiency and also shorten the length of the flame zone.

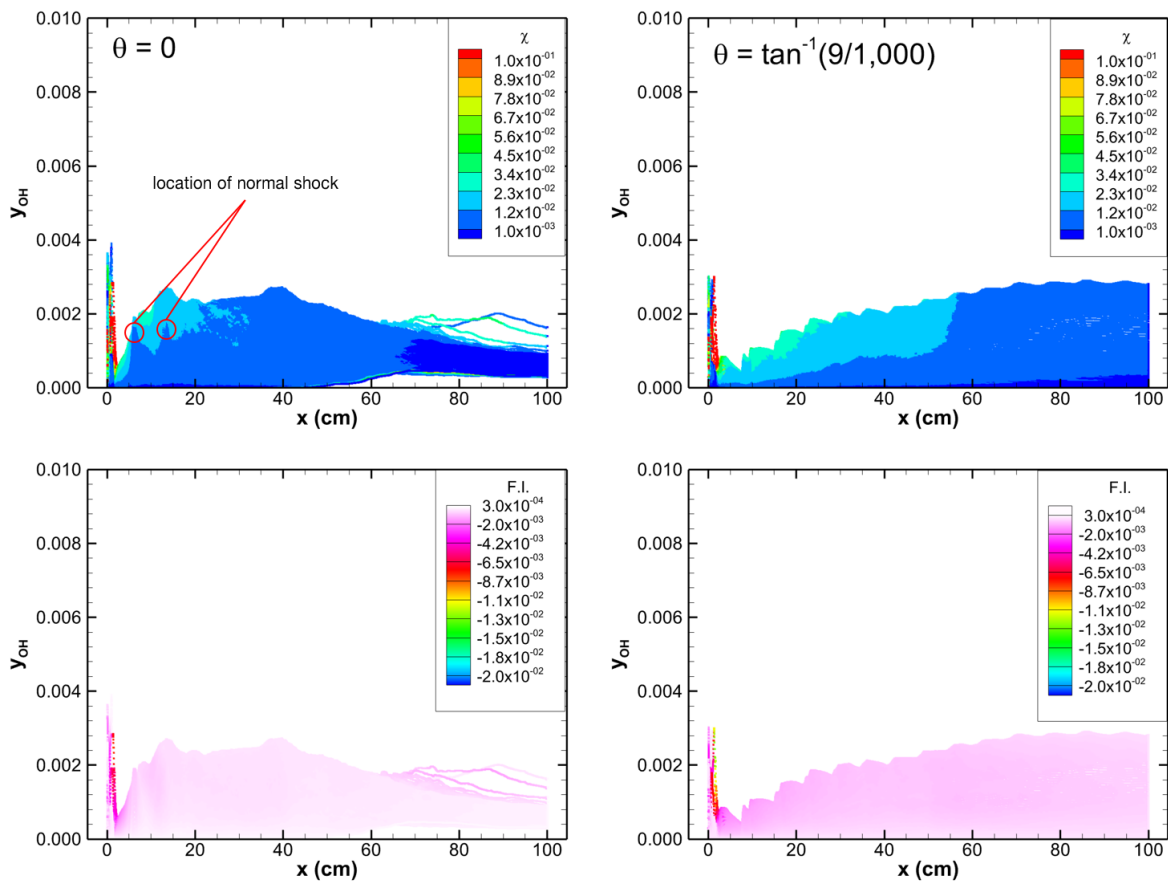


**Fig 7.** Scatter plots of time-averaged OH mass fraction as a function of the x-axis colored by (top) scalar dissipation rate (SDR,  $\chi$ ) and (bottom) flame index (FI) for the cases of  $\theta=0$  and  $\tan^{-1}(9/1,000)$

Figure 8 is the results of FFT (Fast Fourier Transform) analysis for time-varying pressure at two locations in the combustors for two extreme cases of  $\theta = 0$  and  $\tan^{-1}(9/1,000)$ , where the amplitude of the case of  $\theta = \tan^{-1}(9/1,000)$  is multiplied by 10 times. It is understood that strength is order of magnitude higher for  $\theta = 0$  with several times lower frequency. It is also understood that the pressure wave generated by the turbulent eddy motion is getting stronger by the combustion enhancement, forming

shock wave occasionally. The strong pressure wave has wider spatial variation and results in low frequency.

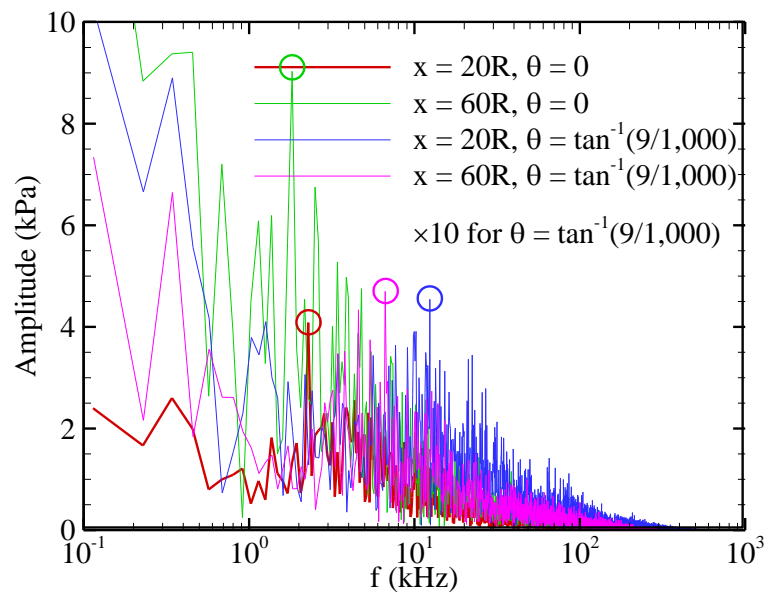


**Fig 8.** FFT frequency analysis of wall pressure at  $x = 20R$  and  $60R$  for the cases of  $\theta=0$  and  $\tan^{-1}(9/1,000)$

#### 4. Conclusion

The simulation for the transient period of thermal choking of the supersonic coaxial combustor is carried out in this study. The results showed that the combustion in DCR exhibit two different combustion modes. The one is the supersonic combustion governed by the turbulent mixing layer, and the other is the stabilization mode by local thermal-choking, which is sustained by the Mach reflection formed by pressure build-up from the combustion heat addition. In this mode, combustion efficiency is further enhanced by the low level of scalar dissipation rate, while total pressure recovery is getting lowered. When the combustion efficiency is enhanced, pressure fluctuation becomes an order of magnitude higher with several times lower frequency due the large spatial motion of the shock waves. Therefore, it is understood that the compressibility effects are fully coupled with the turbulent structures of reacting flows, i.e. shock wave is formed by combustion, while the combustion is enhanced by shock wave, as is in detonation phenomena.

#### Acknowledgement

This research was supported by the Basic Research Program(No. 08-201-501-014) of the Agency for Defense Development(ADD), funded by the Defense Acquisition Program Administration(DAPA) of the Korean Government.

## References

1. Mehta, U.B., "Aerospace America", Vol. 12, 2008, pp. 110-111.
2. Hank, J.M., Murphy, J.S. and Mutzman, R.C., "The X-51A Scramjet Engine Flight Demonstration program" AIAA 2008-2540, 2008.
3. Billig, F.S., Waltrup, P.J., and Stockbridge, R.D., "Integral-Rocket Dual-Combustion Ramjets: A new propulsion concept," Journal of Spacecraft, Vol. 17, No.5, 1980, pp. 416-424.
4. Driscoll, J.F., Huh, H., Yoon, Y., and Donbar, J., "Measured lengths of supersonic hydrogen-air jet flames compared to subsonic flame lengths and analysis", Combustion and Flame, Vol.107, No.1-2,1996, pp. 176-186.
5. Yu, K.H., and Schadow, K.C., "Cavity-actuated supersonic mixing and combustion control", Combustion and Flame, Vol.99, No.2, 1994, pp.295-301.
6. Roy, C.J. and Edwards, J.R., "Numerical simulation of a three-dimensional flame/shock wave interaction", AIAA Journal, Vol.38, No.5, pp.745-754.
7. Kim, J. H., Yoon, Y., Jeung, I.-S., Huh, H., and Choi, J.-Y., "Numerical Study of Mixing Enhancement by Shock Waves in Model Scramjet Engine," AIAA Journal, Vol. 41, No. 6, 2003, pp.1074-1080.
8. Singh, D. J., and Jachimowski, C.J., "Quasiglobal Reaction Model for Ethylene Combustion," AIAA Journal, Vol. 32, No. 1, 1994, pp.213-216.
9. Choi, J.-Y., Yang, V. and Ma., F., " High Resolution Numerical Study on the Supersonic Turbulent Flame Structures and Dynamics in Dual Combustion Ramjet," AIAA Paper 2014-3744, AIAA Propulsion Energy Forum 2014, Cleveland, Ohio (2014).
10. Choi, J.-Y., Han, S.H., K.H. Kim, and Yang, V., "Numerical Study of the Coaxial Supersonic Turbulent Combustion, Part I: Validation Case," AIAA 2014-3745, AIAA Propulsion Energy Forum 2014, Cleveland, Ohio, 2014.
11. Peters, N., Turbulent Combustion, Cambridge University Press, U.K., 2000.
12. Yamashita, H., Shimada, M., and Takeno, T, "A Numerical Study on Flame Stability at the Transition Point of Jet Diffusion Flames," Proceedings of the Combustion Institute, Vol. 26, No. 1, 1996, pp.27-34.